

EUCLID: ESA'S DARK ENERGY 3-AXIS STABILIZED SURVEY MISSION AT THE NIGHT-SIDE SUN-EARTH LIBRATION POINT

Florian Renk⁽¹⁾ and Markus Landgraf⁽²⁾

⁽¹⁾⁽²⁾European Space Operations Centre, European Space Agency, Robert-Bosch-Str. 5,
64293 Darmstadt, Germany, +49-6151-90-2443, Florian.Renk@esa.int /
Markus.Landgraf@esa.int

Abstract: *The Euclid dark energy mission is one of the future missions in the framework of the ESA Cosmic Vision Programme 2015-2025. The mission's purpose is to map about $15,000^{\circ 2}$ of the sky region with galactic latitudes above 30° and free of extinction in an effort to observe how weak gravitational lensing affects the shape of distant galaxies. The operational orbit of Euclid will be a quasi-Halo orbit about the night side Sun-Earth Libration Point (SEL 2). Unusual for a survey mission, the spacecraft will be 3-axis stabilized and scan the sky with a field of view of about $0.5^{\circ 2}$ in a step-and-stare mode, implemented by a hybrid attitude control system consisting of reaction wheels and cold gas thrusters in order to fulfil the high absolute pointing stability. The launch is envisioned on a Soyuz-Fregat from ESAs spaceport in Kourou, French Guiana. We will describe the general mission analysis and the launch window design together with the treatment of perturbations on the trajectory caused by the step-and-stare implementation of the sky survey requiring the use of cold gas thrusters. This is necessary to reduce the station-keeping ΔV allocation, which is a major part of the propellant budget.*

Keywords: *Euclid, Libration Point, Lagrange Point, Mission Analysis, Mission Design*

1. Introduction

Euclid is an ESA mission to map the space-time geometry of the dark universe. The mission will investigate the distance-redshift relationship and the evolution of cosmic structures by measuring shapes and redshifts of galaxies and clusters of galaxies out to redshifts ~ 2 , equivalent to a look-back time of 10 billion years. In this way, Euclid will cover the entire period over which dark energy played a significant role in accelerating the expansion. Euclid will map the 3D distribution of up to two billion galaxies and dark matter associated with them, spread over most of the sky. Thus, the mission will map the large-scale structure of the Universe over most of the extragalactic sky - about half of the full sky excluding the regions dominated by the stars in our Milky Way. The region to be covered corresponds to about $15,000^{\circ 2}$.

The mission is optimised to tackle some of the most important questions in modern cosmology: How did the Universe originate and why is it expanding at an accelerating rate, rather than slowing down due to the gravitational attraction of all the matter in it?

Euclid is optimised for two primary cosmological probes:

Weak gravitational Lensing (WL) Weak lensing is a method to map the dark matter and measure dark energy by measuring the distortions of galaxy images by mass inhomogeneities along the line-of-sight.

Baryonic Acoustic Oscillations (BAO) BAOs are wiggle patterns, imprinted in the clustering of galaxies, which provide a standard ruler to measure dark energy and the expansion in the Universe.

Weak gravitational lensing requires extremely high image quality because possible image distortions by the optical system must be suppressed or calibrated-out to be able to measure the true distortions by gravity.

To provide Euclid with a stable thermal environment, limited communication distance and a large part of the sky unobstructed from the Sun, Earth and the Moon a quasi-halo orbit was chosen as the operational orbit. The 3-axis stabilization of Euclid allows to use a communication system that does not require an amplitude reduction manoeuvre and thus the S/C is transferred to its operational orbit via a so called free-transfer. This transfer strategy together with the launch window calculation and the associated constraints will be presented in Section 3. of this paper.

Besides the transfer the orbit maintenance is of special interest for the Euclid mission design, since the station-keeping ΔV can be a significant part of the total ΔV budget. With almost no deterministic manoeuvres the propulsion system design will mainly be driven by the stochastic processes during launch, the accuracy of the manoeuvre execution and the perturbation level when in the operational orbit. The high image quality requires a very high absolute pointing stability of the spacecraft. This, together with the step-and-stare survey, causes a dilemma in the design of the attitude control system of the S/C. While the jitter caused by the available reaction wheels is too strong to fulfill the absolute pointing requirements, the use of cold gas thruster is very demanding with respect to consumables when considering the number of pointings required to cover the $15,000^{\circ 2}$ with a FoV of about $0.5^{\circ 2}$ and some required overlap. A hybrid system was thus proposed for Euclid using reaction wheels for the slews between the individual pointings, stopping the wheels and compensating any perturbation torques utilizing the cold gas system during a science observation. This compensation of the torques causes a residual ΔV on the operation orbit of Euclid, which can be significantly amplified due to the inherent instability of orbits about the collinear libration points. This station-keeping issue will be addressed in Section 5.

2. Libration Point Orbits

Libration Points exist in a system of two massive celestial bodies orbiting each other. These bodies are referred to as the primaries or primary and secondary, with the larger and smaller mass, respectively. This section gives an introduction to the motion in the vicinity of a libration point orbit. A more detailed analysis can be found in [1, 2]. As an approximation of the real system we use the circular restricted three-body problem (CR3BP), assuming that the primary and secondary body are on circular orbits. The rotating coordinate frame, having its origin in the barycenter of the two bodies, is defined with the x -axis pointing from the primary body to the secondary, e.g. the Sun to the Earth, the z -axis pointing in the direction of the orbit normal and the y -axis supplementing the system to be a right hand one. The well known equation of motion of a third massless body in

the CR3BP [3, 4] can be written as

$$\begin{aligned}\ddot{x} - 2\dot{y} &= U_x, \\ \ddot{y} + 2\dot{x} &= U_y, \\ \ddot{z} &= U_z.\end{aligned}\tag{1}$$

The distances and velocities are normalized by the distance between the primaries and their angular velocity, respectively, and the effective potential U is:

$$U = \frac{1-\mu}{r_1} + \frac{\mu}{r_2} + \frac{1}{2}(x^2 + y^2)\tag{2}$$

with $\mu = \frac{m_2}{m_1+m_2}$ and m_1, r_1 and m_2, r_2 being the masses and distance of the S/C from primary and secondary, respectively. The general solution for the collinear points can then be written as

$$\begin{aligned}x &= A_1 e^{\lambda_{xy} t} + A_2 e^{-\lambda_{xy} t} + A_3 \cos \omega_{xy} t + A_4 \sin \omega_{xy} t, \\ y &= c_1 A_1 e^{\lambda_{xy} t} - c_1 A_2 e^{-\lambda_{xy} t} + c_2 A_4 \cos \omega_{xy} t - c_2 A_3 \sin \omega_{xy} t, \\ z &= A_z \cos(\omega_z t + \Phi_z)\end{aligned}\tag{3}$$

with the constants $c_1, c_2, \lambda_{xy}, \lambda_z, \omega_{xy}$ and ω_x solely depending on the mass parameter μ and the integration constants A_1, A_2, A_3, A_4 and Φ_z depending on the initial conditions of the system.

This solution gives a good idea of the motion of a libration point orbit and also about a transfer strategy. The initial conditions \vec{x}_0 can be selected in such a way that only the oscillatory mode with the amplitudes A_3, A_4 and A_z are excited. The exponential terms are then not involved in the solution and we have two oscillations with slightly different frequencies, one in the xy -plane and one in the z -direction. For the in- and out-of-plane motion the amplitudes $A_x, A_y = c_2 A_x$ and A_z can be calculated. The resulting trajectory in the rotating frame is a Lissajous figure, hence, these orbits are called Lissajous orbits. The two exponential terms, represented by the so called "stable" and "unstable" manifolds, which are "tubes" in space leading to, or departing from the libration point orbit. In the case of the Sun-Earth system, initial conditions close to Earth can be found where only the oscillatory mode and the exponentially decreasing term are excited. The S/C will then travel towards the libration point orbit on the tube of the stable manifold, resulting in a so called "free-transfer"-trajectory, since due to the decreasing exponential component the motion of the S/C will eventually be dominated by the oscillatory modes without further manoeuvres [5]. In the case of the Earth-Moon system such initial conditions do not exist. Some of the manifolds do again approach the secondary body (Moon), but not the primary body (Earth). The transfer trajectory options are discussed in [6].

The solution to the equations of motion as provided in Equations 3 is based on the linearized equations of motion of the CR3BP and is therefore only valid in the vicinity of the associated

libration point. For large libration point orbit amplitudes the non-linear effects will have to be taken into account. Since a numerical propagation in a realistic system, e.g. taking the eccentricity and third body perturbations into account, will always deviate from this solution, a set of "osculating Lissajous elements" $[A_1, A_2, A_x, A_z, \Phi_{xy}, \Phi_z]$ can be defined similar to the "osculating Kepler elements" [7]. The following relationship allows for their calculation at a given epoch (setting $t = 0$):

$$\begin{aligned}
x &= A_1 e^{\lambda_{xy}t} + A_2 e^{-\lambda_{xy}t} + A_x \cos(\omega_{xy}t + \Phi_{xy}), \\
y &= c_1 A_1 e^{\lambda_{xy}t} - c_1 A_2 e^{-\lambda_{xy}t} - c_2 A_x \sin(\omega_{xy}t + \Phi_{xy}), \\
z &= A_z \cos(\omega_z t + \Phi_z), \\
\dot{x} &= A_1 \lambda_{xy} e^{\lambda_{xy}t} - A_2 \lambda_{xy} e^{-\lambda_{xy}t} - A_x \omega_{xy} \sin(\omega_{xy}t + \Phi_{xy}), \\
\dot{y} &= c_1 A_1 \lambda_{xy} e^{\lambda_{xy}t} + c_1 A_2 \lambda_{xy} e^{-\lambda_{xy}t} - c_2 A_x \omega_{xy} \cos(\omega_{xy}t + \Phi_{xy}), \\
\dot{z} &= -A_z \omega_z \sin(\omega_z t + \Phi_z).
\end{aligned} \tag{4}$$

Perturbations on the trajectory will always cause a small A_1 component to exist, making the collinear libration point orbits unstable.

2.1. Escape and Non-escape Direction in the Linear Problem

Assuming a manoeuvre $\Delta\vec{v} = (\Delta\dot{x}_0, \Delta\dot{y}_0, 0)$ in the xy -plane is executed at a point $\vec{x}_0 = (x_0, y_0, z_0, \dot{x}_0, \dot{y}_0, \dot{z}_0)$ on a libration point orbit results in the new amplitudes \hat{A}_1 and \hat{A}_2 [7]:

$$\begin{pmatrix} \hat{A}_1 \\ \hat{A}_2 \end{pmatrix} = \begin{pmatrix} \frac{c_2 \omega_{xy}}{2d_1} & \frac{\omega_{xy}}{2d_2} & -\frac{c_2}{2d_2} & \frac{1}{2d_1} \\ \frac{c_2 \omega_{xy}}{2d_1} & -\frac{\omega_{xy}}{2d_2} & \frac{c_2}{2d_2} & \frac{1}{2d_1} \end{pmatrix} \begin{pmatrix} x_0 \\ y_0 \\ \dot{x}_0 + \Delta\dot{x}_0 \\ \dot{y}_0 + \Delta\dot{y}_0 \end{pmatrix}. \tag{5}$$

Starting from a state vector \vec{x}_0 which satisfies $A_1 = 0$, any velocity increment $\Delta\vec{v} = (\Delta\dot{x}_0, \Delta\dot{y}_0)$ in the xy -plane which satisfies $\vec{u}^T \Delta\vec{v} = 0$ with

$$\vec{u} = \begin{pmatrix} -\frac{c_2}{d_2} \\ \frac{1}{d_1} \end{pmatrix} \tag{6}$$

will not lead to an escape from the family of orbits with periodic components only. \hat{A}_1 remains zero and the \hat{A}_2 component will exponentially decay. The periodic z -motion remains unaffected. The

vector \vec{u} defines the **escape direction** while the vector

$$\vec{s} = \begin{pmatrix} \frac{1}{d_1} \\ \frac{c_2}{d_2} \end{pmatrix} \quad (7)$$

in the xy -plane orthogonal to \vec{u} defines the **non-escape direction**.

The escape direction is important for the numerical construction of non-escape orbits about the collinear libration points, while the non-escape direction is important for manoeuvres changing the amplitude of the orbit as well as eclipse and occultation avoidance.

2.2. Classification of Libration Point Orbits

To investigate transfer trajectories it is of course important to know the final conditions at the destination. It is not sufficient to just specify an arbitrary libration point orbit as destination, since several different types of orbits with specific properties exist. These orbits will deviate significantly from the linear solution derived in Equation 3, but the osculating Lissajous elements as defined in Equation 4 still remain meaningful, even for orbits with a large deviation from the solution of the linearized equations of motion. From literature [8] four different kinds of orbits are known to exist in the Sun-Earth and the Earth-Moon system. In the scope of this work they are defined as follows:

Lyapunov Orbits are planar orbits that have no out-of-plane motion and that entirely lie in the orbital plane of the primaries.

Lissajous Orbits are defined to be orbits with an in- and out-of-plane oscillation. However, the frequencies of the oscillation of the in- and out-of-plane motion differ. Lissajous orbits can be seen as quasi-symmetric to the xy -plane and the xz -plane.

Halo Orbits also have an in- and out-of-plane motion, but here the frequencies are equal and therefore the orbits are periodic. The symmetry to the xy -plane of the primaries does not exist anymore. Halo orbits only exist for a minimum in-plane amplitude and provide an exclusion zone about the line connecting the primaries.

Quasi-Halo Orbits are a "mixture" of Lissajous and Halo orbits. Quasi-Halo orbits originate from Lissajous orbits from a certain minimum boundary value of the out-of-plane amplitude. At this boundary amplitude the Lissajous orbits lose their symmetry with respect to the xy -plane and start to develop an exclusion zone about the line connecting the primaries.

3. Euclid Launch Window Calculation

Euclid being a three-axis stabilized spacecraft does in general not pose any restrictions on the size of the libration point orbit due to the possibility of a high gain communication system. The Euclid

spacecraft design is depicted in Figure 1. The S/C can simplified be treated as consisting of three components:

- Service Module
- Payload Module
- Sunshield

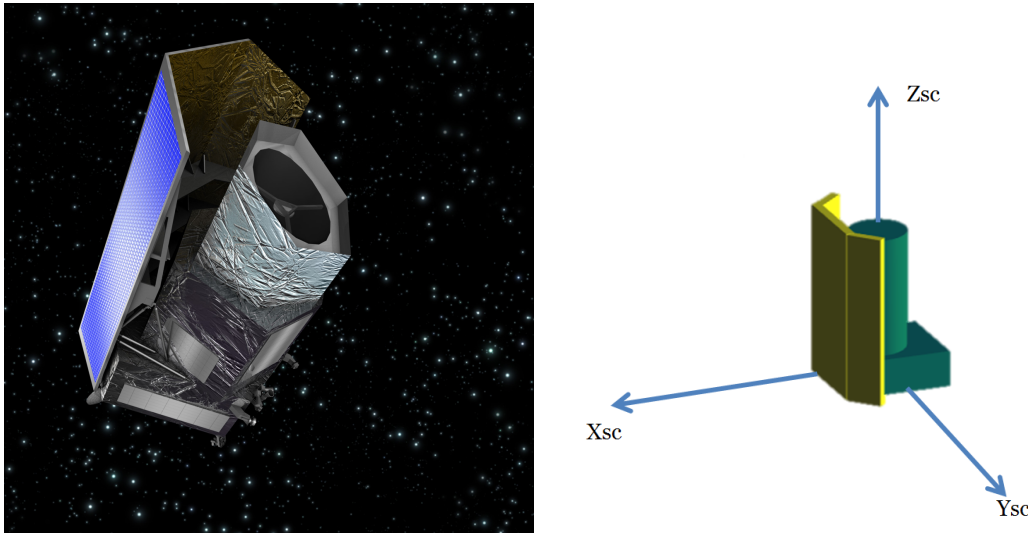


Figure 1. Euclid spacecraft artist impression (Copyright ESA) (left) and Euclid body axis definition (right).

Large libration point orbits have the feature of having a stable manifold that intersects with the vicinity of Earth as it can be seen in Figure 2.

This means that a launch vehicle can theoretically inject the S/C directly into a transfer towards one of the collinear libration point orbits without further manoeuvres by the S/C. In the real transfer scenario an injection close to this ideal condition is desirable, but limited due to several constraints. These constraints define the launch window of the S/C and will be detailed in this section.

- Impact of the Moon on the required apogee altitude / perigee velocity
- Launcher dispersion
- Maximum ΔV /propellant allocation
- Illumination constraints during the launcher ascent phase
- Orbit amplitude constraints

3.1. Launch Scenario from Kourou

One feature Euclid has in common with most other space projects is the mass criticality even before the S/C has been built. In order to achieve the best utilization of the envisioned Soyuz-Fregat launcher a maximum performance launch from Europe's spaceport in Kourou is planned. This maximum performance launch must propel the payload to almost parabolic velocity. As interface point an apogee altitude of $1.5 \cdot 10^6$ km is usually defined. The ascent optimization yields a trajectory

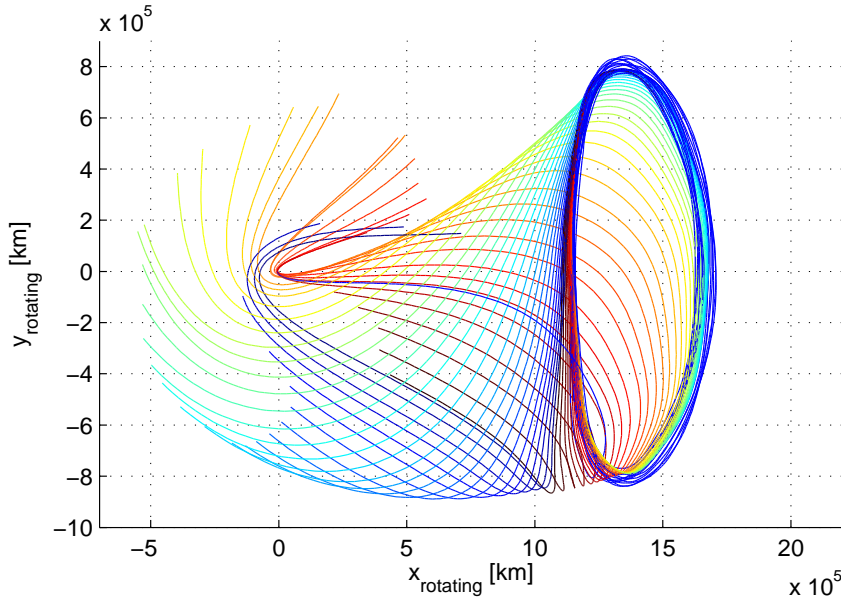


Figure 2. Stable Manifold of Euclid example operational orbit and transfer trajectory. The stable manifold passes nearby the Earth, which is located at the origin of the plot.

without an intermediate coast arc and without an intermediate parking orbit. Since this trajectory is fixed with respect to the Earth the launch time can be used to point the line of apses into the correct direction (towards SEL2). This is shown in Figure 3, where for different launch times the resulting transfer trajectories and their corresponding orbits are depicted. The size of a resulting libration point orbit can be measured by its amplitudes, but also by the Sun-S/C-Earth (SSCE) angle, which is an important geometric property for the communication system design.

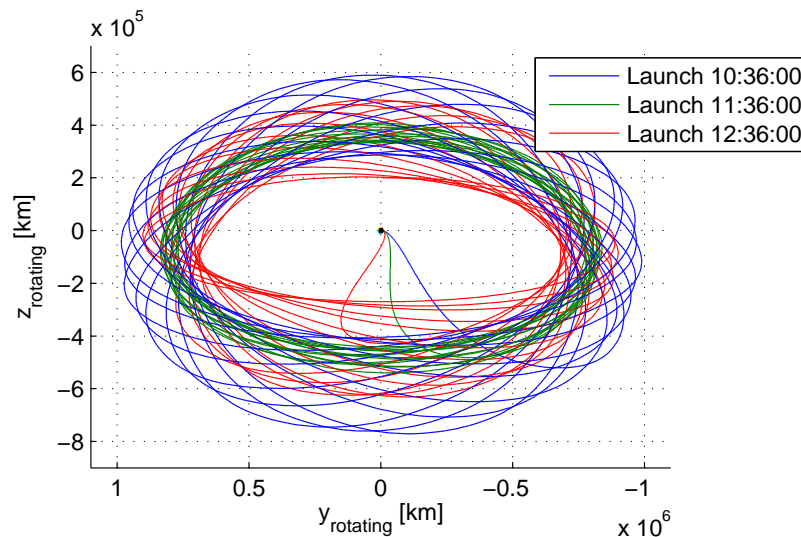


Figure 3. Resulting quasi-Halo orbit shapes and sizes for three different launch times.

A transfer towards the SEL2 can only be established in a specific region for the perigee. As it can also be seen, the size of the resulting libration point orbit will also depend on the launch time. The full unconstrained launch window is shown in Fig. 4.

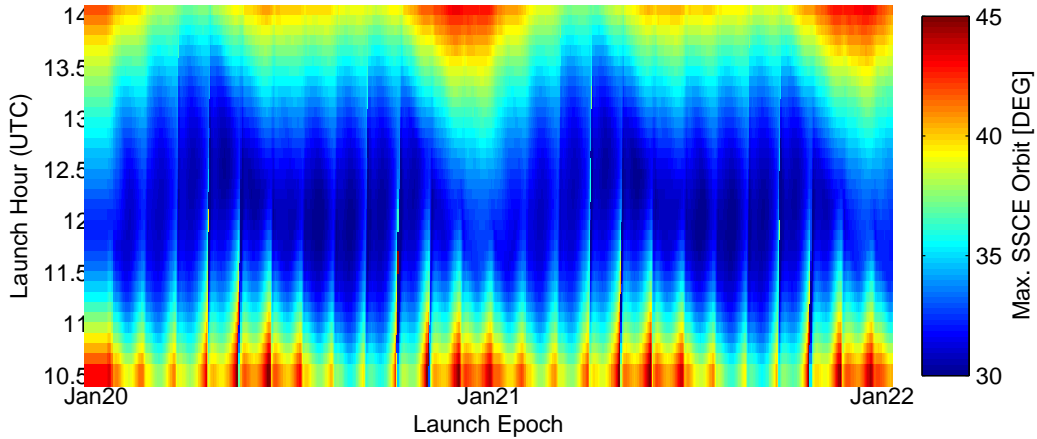


Figure 4. Size of the resulting libration point orbit for different launch times and dates. Constraints have not been applied.

However, unfortunately the launcher cannot directly achieve this unconstrained launch window. The perigee velocity or apogee altitude required for these transfers on the stable manifold does not necessarily match the velocity delivered by the launch vehicle, which is fixed. Thus, a manoeuvre must match the velocity after separation from the launcher to the velocity of the stable manifold. The variation in the perigee velocity over the launch window is depicted in Fig. 5.

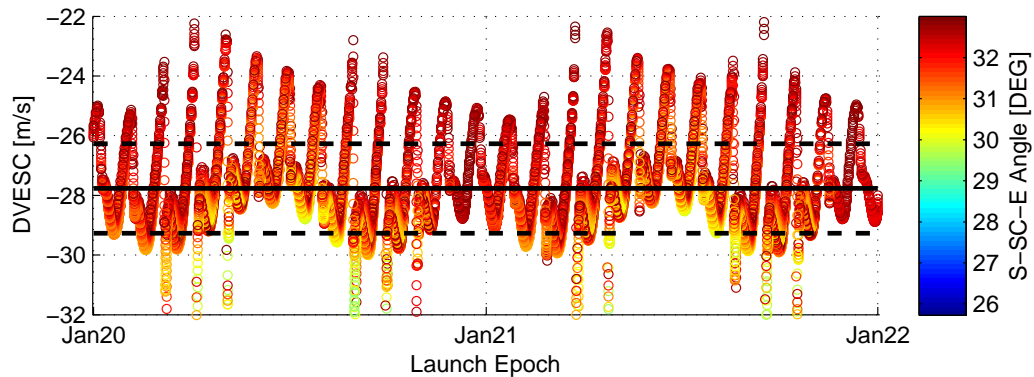


Figure 5. Required perigee velocity for an insertion onto the stable manifold of an SEL2 orbit at the separation point of the launch vehicle. The solid black line represents the velocity targeted by the launch vehicle and the dashed black lines represent the deviation in the velocity that can be covered by the S/C by a manoeuvre.

Several features can be identified from Fig. 5. A daily variation exist to insert the S/C on different local manifolds (compare Fig. 3). A monthly variation exists due to the influence of the moon. Once a month, when the moon crosses the region of the transfer trajectories, the perigee velocity shows two peaks. First, the perigee velocity increases and then the perigee velocity decreases. The effect could be describes as a weak fly-by decelerating or accelerating the S/C and thus it initially requires are larger or lower velocity to reach the same apogee altitude after crossing the lunar region. A seasonal variation can be observed as well. This seasonal variation is a result of the 23.5° tilt of the Earth's rotation axis with respect to the ecliptic plane. Since the launcher ascent trajectory is

fixed with respect to the Earth's equatorial axis, the motion of the Earth in its orbit around the Sun will cause the line of apses of the transfer orbit to have a different declination with respect to the ecliptic plane. In winter the initial transfer orbit will be high above the ecliptic plane, around the solstices the transfer will be close to the ecliptic plane in summer the initial transfer arc will be in the southern ecliptic hemisphere. The passing of the line of apses near the ecliptic plane can also be seen by the strong excursions of the perigee velocity in Fig. 5 caused by the closer approach to the moon, whose orbit is only slightly inclined with respect to the ecliptic plane.

As mentioned before, this variation in the perigee velocity must be compensated by a manoeuvre. However, the manoeuvre cannot take place at perigee, since the perigee is only a virtual state, the S/C is separated with a true anomaly different from zero. But there are other reasons that prohibit an early execution of this correction manoeuvre. The first reason is the unknown launcher dispersion. After separation from the upper stage the actual achieved orbit must be estimated by using radiometric measurements. Then the correction manoeuvre can be calculated combined with the perigee velocity correction and uploaded to the S/C. It can be expected that an execution of the manoeuvre can be performed about 24 h into the mission, but to also account for contingencies an execution on day 2 is budgeted. The problem with the deviation in the perigee velocity is the amplification of this deviation over time. Since the primary objective of the manoeuvre is the adjustment of the apogee altitude and thus correcting the semi-major axis, the manoeuvre is most efficient when the S/C is travelling fast. But after two days of drifting away from the Earth the S/C will have significantly slowed down. Fig. 6 shows the theoretical amplification of a perigee velocity deviation over time.

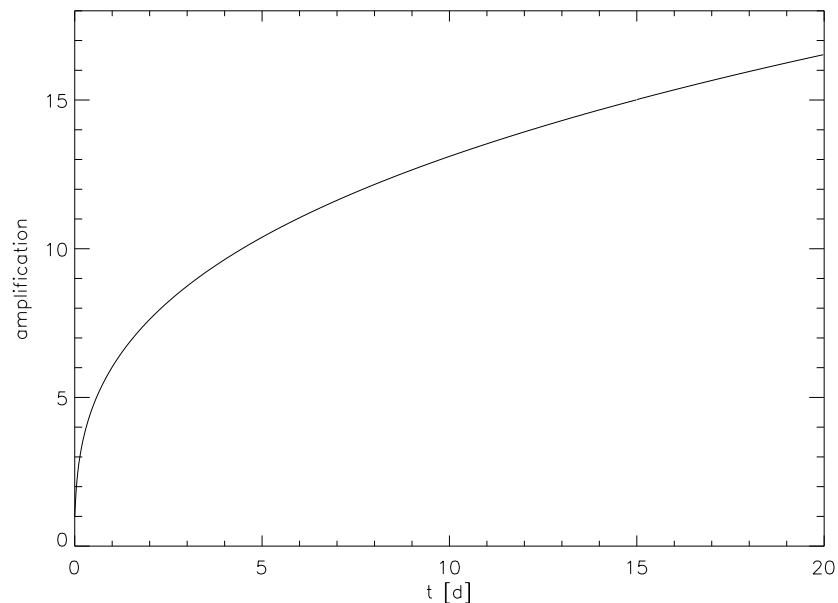


Figure 6. Amplification of the tangential velocity error due to the dynamics on a parabolic escape trajectory.

As it can be seen from the figure, the amplification factor has reached a value of about 8 after two days. Coming back to Fig. 5 one can see that the interval of perigee velocities is about 10 m/s.

Setting the launcher to inject at the center of the interval leaves 5 m/s to be corrected in each direction. Amplified by a factor of eight would result in a ΔV of 40 m/s for the nominal correction to which the launcher dispersion must be added.

To limit the ΔV allocation on the S/C the full interval of perigee velocities is not covered, but only a perigee velocity deviation of ± 1.5 m/s. This limitation imposes a launch window constraint. The virtual perigee velocity targeted by the launcher is optimized to maximize the number of consecutive launch days available after taking further constraints into account. This velocity together with the covered interval can be seen in Fig. 5.

The launch window with the optimized injection velocity and adhering to the ± 1.5 m/s constraint is depicted in Figure 7. The separation into monthly launch windows can be clearly seen.

3.2. Sun-Spacecraft-Earth Angle Constraint

In general any large amplitude quasi-Halo orbit could be used for Euclid, but for a couple of reasons it is desirable to limit the size of the SEL2 orbit. The three main reasons are:

- Definition of a maximum antenna-Earth angle for the design of the communication module
- Maximum and minimum ground station visibility will strongly depend on the orbit size
- Independence of the planned Euclid Sky Survey from the SEL2 orbit

Based on the three items above a maximum Sun-S/C-Earth angle of 33° should not be exceeded. When applying the constraint to the previously presented unconstrained launch window the situation changes as depicted in Fig. 7.

3.3. Eclipses

A further constraint that must be applied to the launch window is to injection into an eclipse free transfer trajectory and operational orbit. As it can be seen from Fig. 7, eclipses do occur around the equinoxes, when the transfer trajectory is close to the ecliptic plane and thus can pass through the Earth's shadow.

3.4. S/C Illumination During the Ascent Phase

The final constraint currently taken into account is the allowed illumination of the S/C during the ascent. In the operational orbit the payload and service module are protected by the Sun shield. During the initial phase of the ascent the S/C is still protected by the launcher fairing, but the fairing cannot remain on the launcher for too long in order to allow for a maximum payload performance delivered into orbit. After the separation of the fairing one situation must be avoided: Direct sunlight entering the telescope. Thus a constraint was imposed that the Sun may not enter a cone around the telescope boresight axis with a half-cone opening angle of 30° . Looking at the ascent trajectory an issue becomes apparent immediately. If the line-of-apses needs to point toward SEL2, the perigee must be on the day side of the Earth. And if the perigee is on the day side of the Earth, the ascent trajectory must be towards the Sun.

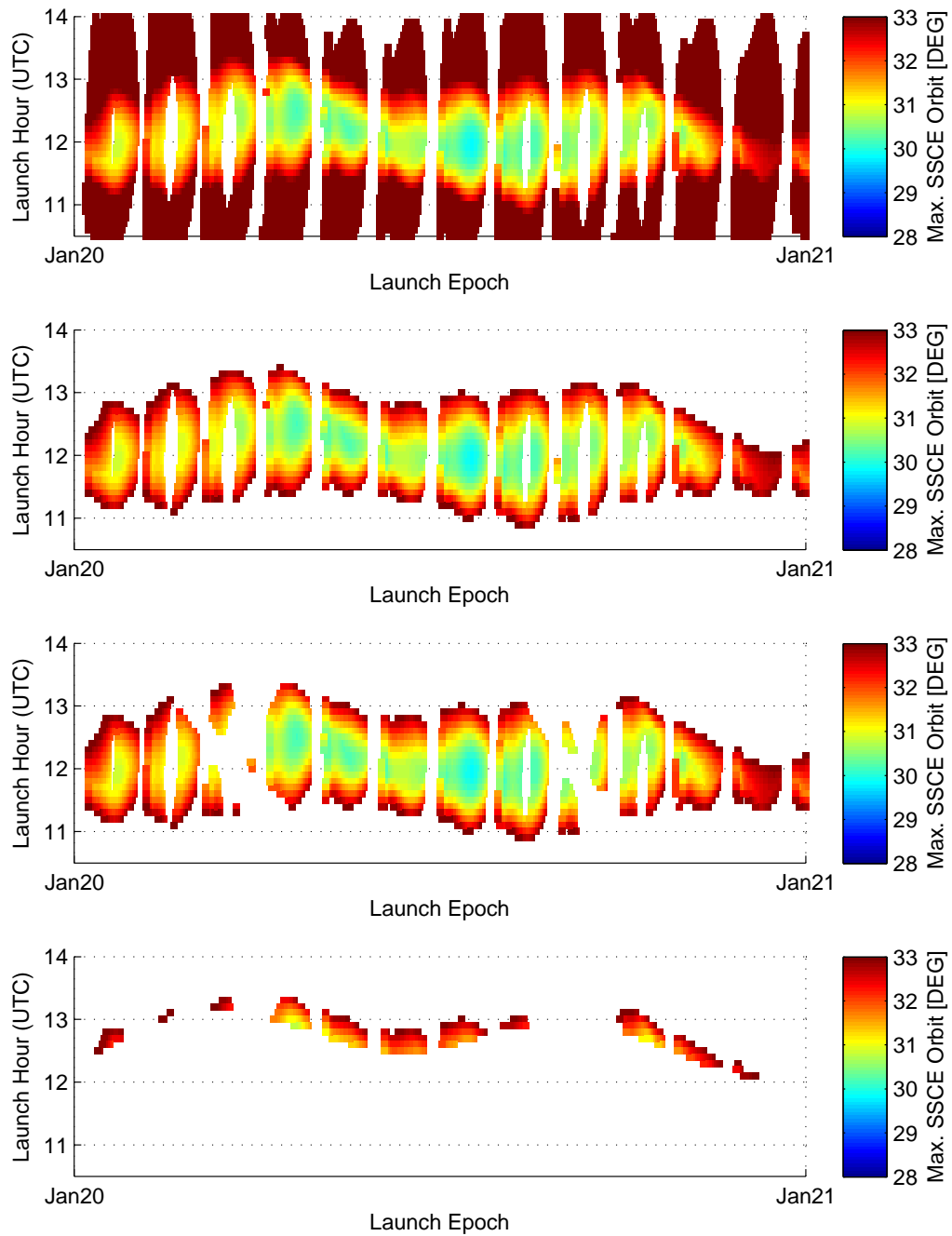


Figure 7. Launch window constraints added from top to bottom: Limitation in perigee velocity, limitation in SSCE angle, exclusion of eclipses and constraining launch time to adhere with illumination constraints during the ascent.

3.5. Remaining Launch Window

Figure 7 depicts the currently remaining launch window when all constraints are applied. To increase the robustness in the winter months a relaxation of the illumination constraint is envisioned. This would allow for earlier launches every day.

4. Transfer Navigation

The aim of the transfer navigation is to inject Euclid into an operational orbit that adheres to all constraints, mainly the constraint on the SSCE angle. The first correction manoeuvre is scheduled about 24 h into the mission, but is budgeted as executed at day-2 to account for contingencies. This first transfer correction manoeuvre (TCM) corrects for the deviation in the required perigee velocity and the launcher dispersion. Manoeuvre execution errors are removed with up to two additional TCMs on day-5 and day-20 (the times can vary). After these three transfer correction manoeuvres the S/C is considered to be on a libration point orbit and the operational orbit is maintained by applying regular station keeping manoeuvres.

5. Staying at SEL2 - Station-Keeping Considerations

Once the science phase of Euclid starts the S/C must be kept in an orbit around SEL2. The station-keeping strategy for Euclid is not to target a reference orbit, but to simply aim for a new non-escape orbit around SEL2 at the scheduled manoeuvre time. This is done by performing manoeuvres in the unstable direction, removing any component in the escape direction that builds up along this motion. Fig. 8 shows the unstable direction vectors for small amplitude orbits. For small amplitude orbits the solution of the linearized system is valid. For quasi-Halo orbits with larger SSCE angle the non-linear terms cause a deviation of the unstable direction from the one derived from the solution of the linear theory, however, the direction is still used. Since a more optimal direction can be found this approach can be considered as being conservative. Since station-keeping manoeuvres interrupt the science phase they should be kept to a minimum. On the other hand the ΔV required for station-keeping does exponentially increase over time. For libration point mission a station-keeping interval of 30 days usually provides a good compromise between science interruption and propellant allocation.

Because any perturbing acceleration into the unstable direction will exponentially increase the perturbations on the trajectory should be kept small in order to limit the station-keeping ΔV . Unfortunately the cold gas system used to provide the pointing stability during a science observation is an unbalanced system. Taking a look at Fig. 1 one can see that the center of pressure and the center of mass are unlikely to fall together. The center of pressure for the solar radiation pressure is somewhere close to the middle of the sun shield. The center of mass is likely to be lower, since the heavy service module is located close to the origin of the coordinate system definition as in Fig. 1. Thus, the solar radiation pressure will generate a torque rotating the S/C around the $-y_{SC}$ axis. As soon as the unbalanced cold gas system provides a torque compensating mainly the solar radiation pressure torque, a ΔV will be generated as well. The direction of this ΔV will depend on the current S/C attitude. Calculating the resulting acceleration and assuming this acceleration as perturbation leads to unreasonable ΔV values and the station-keeping ΔV would dominate the ΔV budget.

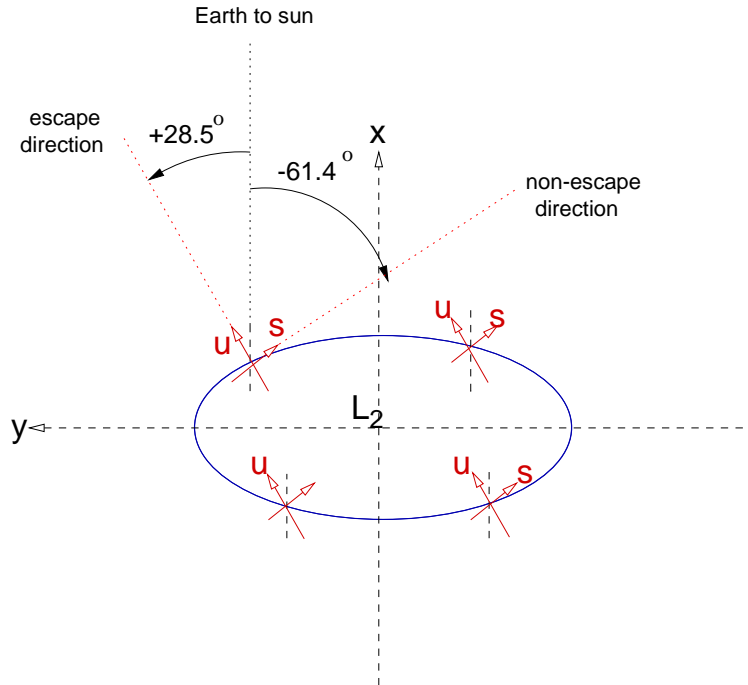


Figure 8. Unstable direction for small amplitude orbits.

In order to lower the ΔV budget the following strategies were proposed:

- Assuming an a-priori known S/C attitude by assuming a known and time fixed sky survey and taking the residual acceleration into account for the orbit design
- Exploiting attitude constraints with common component estimation and trajectory biasing
- Projection of the perturbation on the unstable direction of the linear problem

The first item is a very attractive option, because the residual acceleration can then be incorporated into the trajectory design and only its noise must be treated as a perturbation. However, an a-priori knowledge of the survey was excluded as too optimistic. Thus, the remaining techniques will be discussed in greater detail. The aim of those strategies will be to limit the peak residual acceleration that can act in the operational orbit, since this is then the worst case to be considered. This is not unrealistic, since e.g. the pointings of an existing reference survey are not at all equally distributed, but the distribution shows a heavy bias into specific directions and thus an averaging over the allowed pointing directions is not allowed.

5.1. Exploiting Attitude Constraints

During the operational orbit the attitude of the S/C is strongly constrained to avoid illumination of the payload module, to keep a thermal balance and to ensure a sufficiently large power supply. In the nominal attitude the x_{SC} -axis is pointing towards the Sun. To make observations the S/C can be rotated freely around the x_{SC} -axis. The telescope z_{SC} -axis may also be rotated 30° around the y_{SC} -axis away from the Sun and 1° towards the Sun. The small rotation toward the Sun is required in order to observe the ecliptic poles independent of the orbital motion on the SEL2 orbit. If the

S/C is not tilted back, a great circle can be scanned by rotating about x_{SC} -axis and if the S/C is tilted backwards a small circle can be scanned. Thus, a spherical segment as shown in Figure 9 can be observed at any given time with respect to the rotating frame. With a known cold gas thruster mounting the generated force can be calculated for all possible S/C attitudes. It immediately becomes apparent that the compensating force always has a component, which common to all nominal S/C attitudes in the co-rotating ecliptic coordinate frame. This force is directed in the $-x_{rotating}$ direction as it can also be seen in Fig. 9.

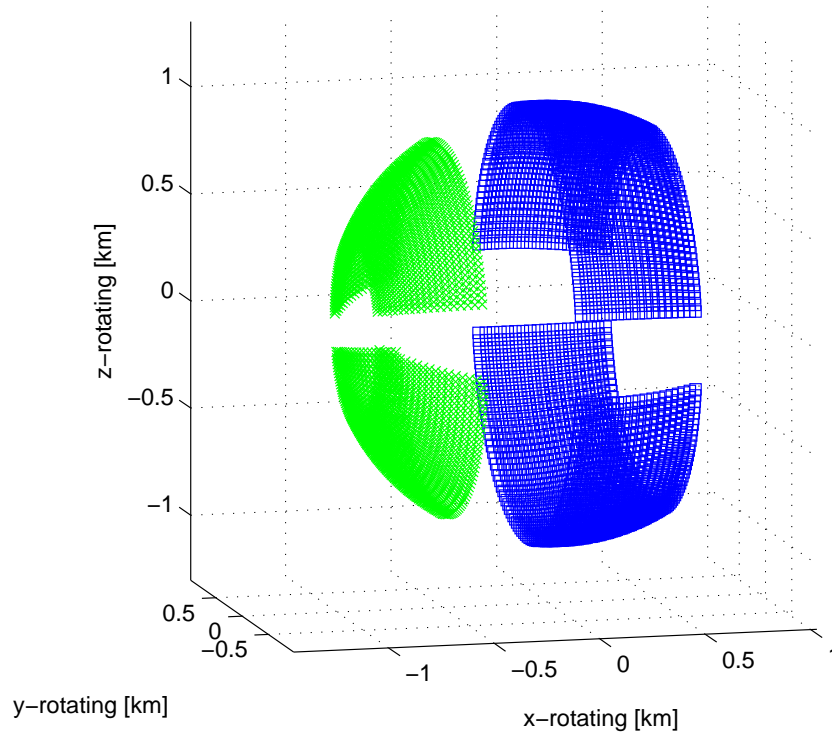


Figure 9. Euclid possible boresight axis pointings (blue squares) and resulting thrust directions (green x) projected on the unit sphere. The S/C will almost never point into the ecliptic plane $\pm 10^\circ$.

A force compensating this common component acting in the $x_{rotating}$ -axis can be generated by biasing the libration point orbit. By shifting the entire libration point orbit along the $x_{rotating}$ -axis, and thus being off-set of the equilibrium point of the three-body problem, will generate a force compensating the common component and thus reducing the overall perturbation force. However, the peaks of this force can be reduced even further, by increasing the bias on the trajectory. With the common component removed the theoretical residual acceleration force will have a component along the $x_{rotating}$ with an interval $[0 a_{max}]$. If the bias is increased beyond removing the common component, the theoretical interval will at one point reach $[-a_{new} + a_{new}]$ with $a_{new} < a_{max}$. This behaviour is schematically depicted in Fig. 10.

The resulting residual force will now be acting in both directions along the $-x_{rotating}$ axis and thus have a component in the $\pm x_{rotating}$ -axis instead of $-x_{rotating}$ only. The effect of the operational orbit

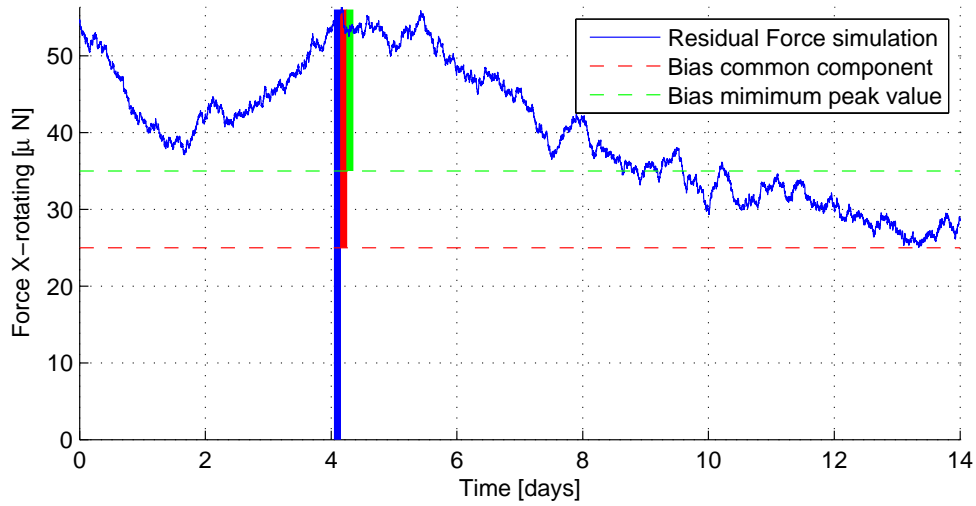


Figure 10. Schematic of removing the common component and reduction of peak force by force biasing. Force biasing is achieved by a shift of the libration point orbit on the $x_{rotating}$ -axis. Biasing is equivalent to shifting the x-axis along the y-axis. The maximum distance from the x-axis to the force curve gives the peak force. By removing the common component only, the theoretical remaining force is only acting in one direction with respect to the new x-axis (red dashed line). If the bias is increased, the theoretical remaining force acts in both directions, the absolute peak value with respect to the new axis (green dashed line) is reduced.

biasing is shown in Fig. 11 with about 1000 times exaggerated accelerations in order to have a visible change in the trajectory.

But what part of this remaining force is important for the station-keeping budget? As shown in Fig. 8 at least for small orbit only components in the unstable direction will be amplified and perturb the orbit. Perturbations out of the ecliptic plane will change the out-of-plane amplitude and phase angle, but will not lead to a departure from the libration point orbit. Components in the stable direction, perpendicular to the unstable one, will exponentially decrease. Thus we have a look at the projection of the remaining force vector on the unstable direction. Fig. 12 again shows the spherical segment of possible pointing vectors in the sky. This time the pointings are color coded. The color represents the projection factor of the residual force on the unstable direction. If the projection factor is 1 the residual force is in the unstable direction, if the factor is 0 the pointing has a residual force in the stable direction. Additionally the plot shows the pointings of a sample survey. The pointings are depicted by the lines originating from the origin.

Unfortunately this knowledge cannot be used to decrease the station-keeping ΔV , since information on the survey shall not be taken into account for the allocation of the station-keeping budget. Thus, it must still be assumed that the major part of the survey pointings are in a direction with a high projection factor.

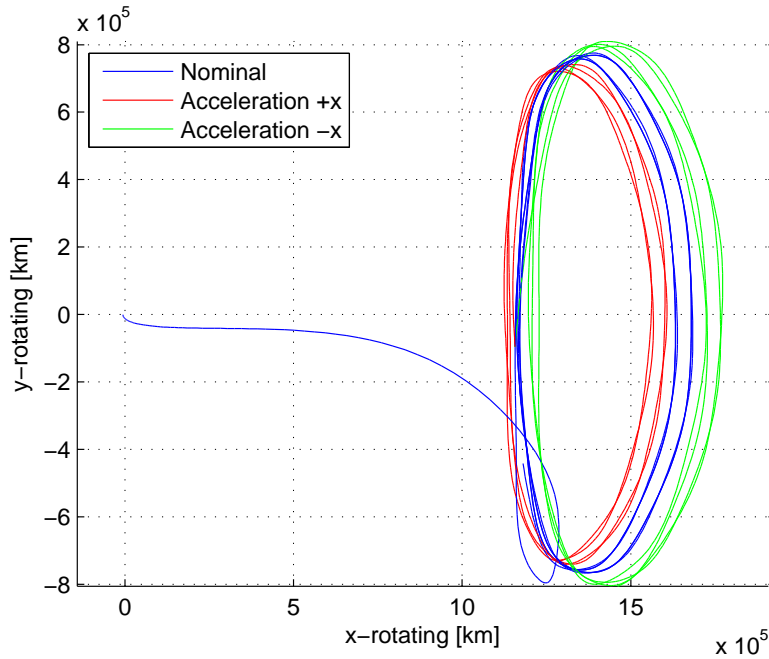


Figure 11. Euclid operational orbit without and with additional acceleration along the $\pm x_{rotating}$ -axis. Acceleration level is $2 \cdot 10^{-8} \text{ km/s}^2$, magnitudes larger than the actual acceleration.

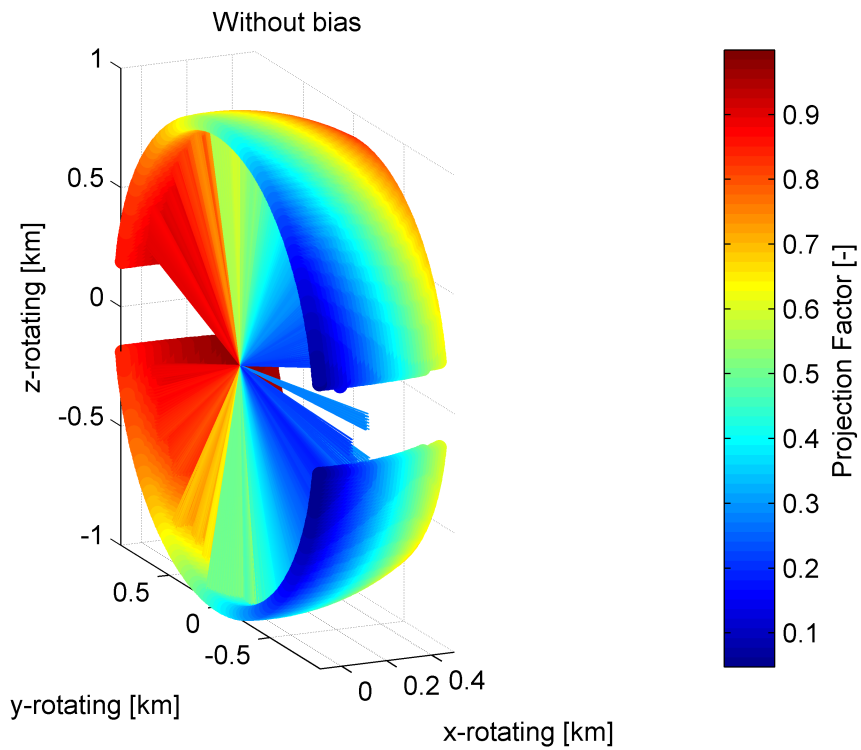


Figure 12. Spherical segment of possible S/C pointings. The color code indicates the component of the compensating force in the unstable direction (factor 1) or into the exponentially decreasing stable direction (factor 0).

5.2. Validity of the Unstable Direction Approximation

In the previous section it was discussed that the station keeping ΔV can possibly be reduced, if only the component of the perturbing force into the unstable direction is considered. However, since Euclid is on a large amplitude quasi-Halo orbit utilizing the unstable direction of the linear problem can only be an approximation. The question arises whether this is a good approximation? This is an important question, when only the projected component shall be taken into account.

To identify how well the unstable direction of the linear theory matches the actual one a typical Euclid quasi-Halo orbit was investigated. An omnidirectional perturbation was added to the nominal state and the amplification of the perturbation was investigated. If the actual unstable direction would match the theoretical one, a perturbation perpendicular to the theoretical one should lead to no required correction and a perturbation in the direction of the theoretical unstable manifold should lead to a maximum in the required correction ΔV . Thus, the required correction plotted with respect to the angle between the theoretical unstable manifold and the perturbation vector should show a cosine graph. Fig. 13 shows this for two different phase angles on the SEL2 orbit. As it can be seen from the Figure the theoretical unstable manifold is a good approximation, but does not always match the actual one. Thus, a penalty factor must be applied to account for the deviation of the actual unstable direction from the theoretical one. This can be seen in Fig. 13, since the maximum absolute penalty value is not reached at 0 or 180°, but at about 25 and 155°.

It can be expected that the deviation increases with increasing orbit amplitudes and thus increasing non-linearities. The orbit size of Euclid is constrained to 33° SSCE angle and thus also the local deviation of the unstable manifold is limited. For the orbits investigated for Euclid the deviation in the force projected onto the unstable direction was several % between the actual and linear theory.

6. Conclusion

The calculation of a valid launch window for Euclid taking all S/C and launcher constraints into account was presented. When utilizing a direct ascent scenario requiring only one Fregat flight program the launch window consists of a block of launch days every months, which are interrupted by the passage of the moon near the transfer trajectory towards SEL2. Around the equinoxes the trajectory is close to the ecliptic plane and thus the launch window closes due to eclipses in the transfer trajectory or the operational orbit. The transfer navigation analysis was conducted to determine preferred manoeuvre directions and to define the required ΔV to reach the operational orbit at SEL2. A strong constraint on the launch window is the minimum angle between the telescope boresight axis and the Sun. If this angle can be decreased a more robust launch window can be achieved.

Due to the utilization of a hybrid attitude control system to achieve a high pointing stability with yet reasonable cold gas consumption a high perturbation level exists and the station-keeping effort is significant. Measures to reduce the required station-keeping ΔV when not taking the sky survey to be conducted into account included the biasing of the orbit to account for a constant common acceleration, additional biasing to lower the peak acceleration force and a projection of the residual force onto the unstable manifold to only account for forces creating an escape from the quasi-Halo

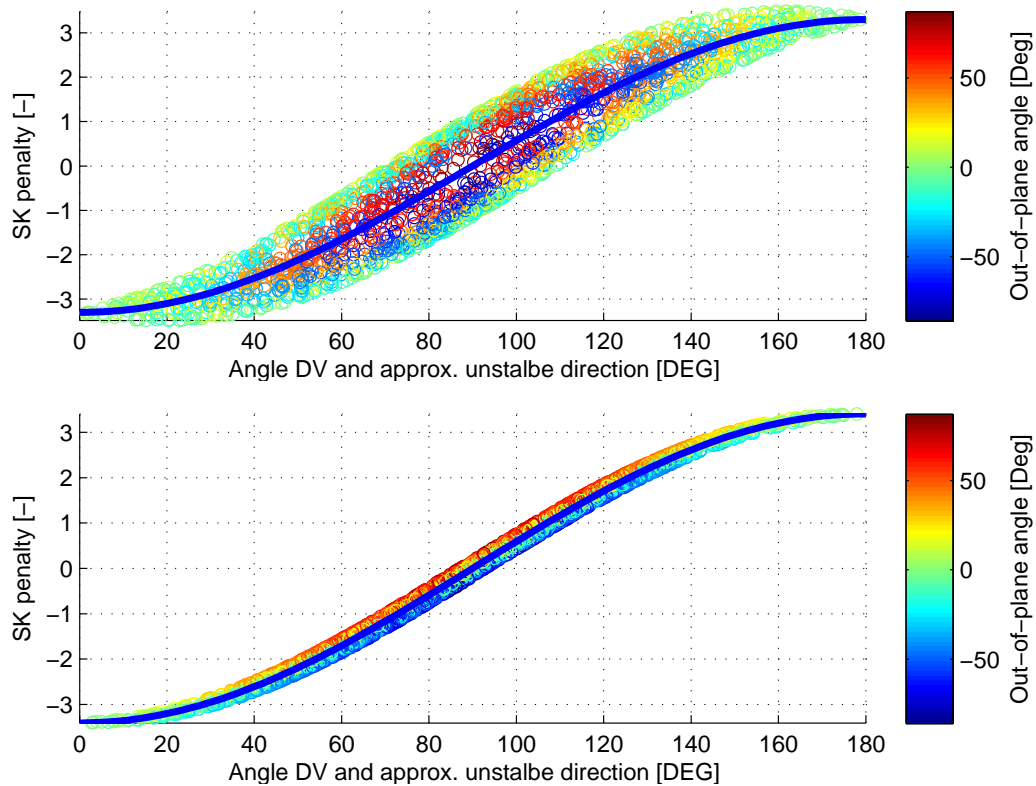


Figure 13. Penalty factor of perturbation ΔV after 30 days with respect to angle between perturbation ΔV and unstable direction vector of the linear theory for two different phase angles on the quasi-Halo orbit (top 130 days into the mission, bottom 174 days into the mission). The blue line represents the cosine curve expected if linear theory was valid.

orbit. Due to the large amplitude quasi-Halo orbit selected for Euclid the maximum deviation of the actual unstable manifold to the one of the linear theory was determined.

Our paper does unfortunately not contain any concrete numbers to not interfere with the current S/C definition between ESA and the prime contractor. If interested the reader is encouraged to contact the authors for numbers once the negotiation phase has been successfully finished.

7. References

- [1] Gomez, G., Masdemont, J. J., and Mondelo, J. M. “Libration Point Orbits: a Survey from a Dynamical Point of View.” “Libration Point Orbits and Applications,” World Scientific Pub Co., 2003.
- [2] Cobos, J. and Masdemont, J. J. “Astrodynamical Applications of Invariant Manifolds Associated with Collinear Lissajous Libration Points.” “Libration Point Orbits and Applications,” World Scientific Pub Co., 2003.
- [3] Farquhar, R. W. The Control and use of Libration-Point Satellites. TR-R 346. NASA, 1970.

- [4] Szebehely, V. Theory of Orbits. Academic Press, New York, 1967.
- [5] Hechler, M. and Yáñez, A. “Herschel/Planck Consolidated Report on Mission Analysis Issue 3.1.” Tech. Rep. PT-MA-RP-0010-OPS-GMA, European Space Operations Centre (ESOC), Darmstadt, 2006.
- [6] Renk, F. “Mission Analysis for Exploration Missions Utilizing Near-Earth Libration Points.” PhD Thesis, Insitute of Space Systems, University of Stuttgart, October 2009.
- [7] Hechler, M. and Cobos, J. “FIRST Mission Analysis: Transfers to Small Lissajous Orbits around L_2 .” MAS Working Paper 398, Mission Analysis Section, ESA/ESOC, July 1997.
- [8] Howell, K. C. “Families of Orbits in the Vicinity of the Collinear Libration Points.” Tech. rep., The Journal of Astronautical Sciences, Vol. 49, No. 1, pp. 107-125, 2001.